

## Energetic Effects of Magnesium in the Recognition of Adenosine Nucleotides by the F<sub>1</sub>-ATPase $\beta$ Subunit<sup>†</sup>

Nancy O. Pulido,<sup>‡</sup> Guillermo Salcedo,<sup>‡</sup> Gerardo Pérez-Hernández,<sup>||</sup> Concepción José-Núñez,<sup>§</sup> Adrián Velázquez-Campoy,<sup>⊥</sup> and Enrique García-Hernández<sup>\*‡</sup>

<sup>‡</sup>*Instituto de Química, and* <sup>§</sup>*Instituto de Fisiología Celular, Universidad Nacional Autónoma de México, Circuito Exterior, Ciudad Universitaria, México 04510, D.F., Mexico,* <sup>||</sup>*Departamento de Ciencias Naturales, Universidad Autónoma Metropolitana-Cuajimalpa, Pedro Antonio de los Santos 84, San Miguel Chapultepec, Miguel Hidalgo, México 11850, Mexico,* and <sup>⊥</sup>*Institute of Bio computation and Physics of Complex Systems (BIFI), Universidad de Zaragoza, Zaragoza, Spain, and* *Fundación ARAID, Diputación General de Aragón, Zaragoza, Spain*

Received April 30, 2010

**ABSTRACT:** Nucleotide-induced conformational changes of the catalytic  $\beta$  subunits play a crucial role in the rotary mechanism of F<sub>1</sub>-ATPase. To gain insights into the energetic bases that govern the recognition of nucleotides by the isolated  $\beta$  subunit from thermophilic *Bacillus* PS3 (T $\beta$ ), the binding of this monomer to Mg(II)-free and Mg(II)-bound adenosine nucleotides was characterized using high-precision isothermal titration calorimetry. The interactions of Mg(II) with free ATP or ADP were also measured calorimetrically. A model that considers simultaneously the interactions of T $\beta$  with Mg·ATP or with ATP and in which ATP is able to bind two Mg(II) atoms sequentially was used to determine the formation parameters of the T $\beta$ –Mg·ATP complex from calorimetric data. This analysis yielded significantly different  $\Delta H_b$  and  $\Delta S_b$  values in relation to those obtained using a single-binding site model, while  $\Delta G_b$  was almost unchanged. Published calorimetric data for the titration of T $\beta$  with Mg·ADP [Pérez-Hernández, G., et al. (2002) *Arch. Biochem. Biophys.* 408, 177–183] were reanalyzed with the ternary model to determine the corresponding true binding parameters. Interactions of T $\beta$  with Mg·ATP, ATP, Mg·ADP, or ADP were enthalpically driven. Larger differences in thermodynamic properties were observed between T $\beta$ –Mg·ATP and T $\beta$ –ATP complexes than between T $\beta$ –Mg·ADP and T $\beta$ –ADP complexes or between T $\beta$ –Mg·ATP and T $\beta$ –Mg·ADP complexes. These binding data, in conjunction with those for the association of Mg(II) with free nucleotides, allowed for a determination of the energetic effects of the metal ion on the recognition of adenosine nucleotides by T $\beta$  [i.e., T $\beta$ ·AT(D)P + Mg(II)  $\rightleftharpoons$  T $\beta$ ·AT(D)P–Mg]. Because of a more favorable binding enthalpy, Mg(II) is recognized more avidly by the T $\beta$ ·ATP complex, indicating better stereochemical complementarity than in the T $\beta$ ·ADP complex. Furthermore, a structural–energetic analysis suggests that T $\beta$  adopts a more closed conformation when it is bound to Mg·ATP than to ATP or Mg·ADP, in agreement with recently published NMR data [Yagi, H., et al. (2009) *J. Biol. Chem.* 284, 2374–2382]. Using published binding data, a similar analysis of Mg(II) energetic effects was performed for the free energy change of F<sub>1</sub> catalytic sites, in the framework of bi- or tri-site binding models.

F<sub>0</sub>F<sub>1</sub>-ATP synthase occupies a prominent place in the repertoire of proteins that specialize in the interconversion of mechanical and chemical energies. Through a sophisticated mechanism involving internal rotary movements, this multimeric enzyme couples the electrochemical potential of protons across membranes to the endergonic synthesis of ATP from ADP and P<sub>i</sub>.<sup>1</sup> The water-soluble F<sub>1</sub> sector ( $\alpha_3\beta_3\gamma\delta\epsilon$ ) carries the enzymatic machinery. In this subcomplex, three  $\alpha$  subunits and three  $\beta$  subunits are arranged alternately, forming a hexagonal ring that encloses part of the elongated  $\gamma$  subunit structure (I). The three catalytic sites of the enzyme are positioned at  $\alpha$ – $\beta$  subunit interfaces, with a large preponderance of  $\beta$  subunit residues. The  $\alpha_3\beta_3\gamma$  oligomer is the minimal construction that preserves

normal rotational and hydrolytic activities (2–4), while the  $\alpha_3\beta_3$  oligomer retains some ATPase activity (5). Dissociation of the  $\alpha_3\beta_3$  oligomer yields natively structured monomeric subunits

<sup>†</sup>This work was supported in part by DGAPA, UNAM (PAPIIT, IN204609), and CONACyT (Grant 47097). N.O.P. and G.S. received fellowships from CONACyT and DGAPA.

\*To whom correspondence should be addressed: Instituto de Química, Universidad Nacional Autónoma de México, Circuito Exterior, Ciudad Universitaria, México 04510, D.F., Mexico. Telephone: +52 55 56 22 44 24. Fax: +52 55 56 16 22 03. E-mail: egarciah@unam.mx.

<sup>1</sup>Abbreviations: Mg(II), free magnesium ion; AMPPNP, adenylyl 5'-imidodiphosphate; P<sub>i</sub>, inorganic phosphate; EDTA, ethylenediaminetetraacetic acid; Tris, 2-amino-2-(hydroxymethyl)propane-1,3-diol; MgCl<sub>2</sub>, magnesium chloride; NaOH, sodium hydroxide; ATPase, adenosine 5'-triphosphatase; T $\beta$ , isolated  $\beta$  subunit from thermophilic *Bacillus* PS3; TF<sub>1</sub>, F<sub>1</sub> sector from *Bacillus* PS3; EF<sub>1</sub>, F<sub>1</sub> sector from *Escherichia coli*; S1–S3, high-, medium-, and low-affinity  $\beta$  subunit sites in F<sub>1</sub>, respectively;  $\beta_{DP}$  and  $\beta_{TP}$ ,  $\beta$  subunits in the crystal structure of F<sub>1</sub> bound to Mg·ADP and Mg·AMPPNP, respectively; ITC, isothermal titration calorimetry; NMR, nuclear magnetic resonance; K<sub>b</sub>, equilibrium binding constant;  $\Delta H_b$ , binding enthalpy;  $\Delta G_b$ , Gibbs binding free energy;  $\Delta S_b$ , binding entropy;  $\Delta C_{pb}$ , binding heat capacity; K<sub>b1</sub> and K<sub>b2</sub>, stepwise association constants for the interaction of ATP with Mg(II); K<sub>p1</sub> and K<sub>p2</sub>, association constants for ATP and Mg·ATP, respectively, binding to T $\beta$ ;  $\Delta H_{int}$ , intrinsic binding enthalpy;  $\Delta H_{dsolv}$ , desolvation enthalpy;  $\Delta S_{conf}$ ,  $\Delta S_{solv}$ , and  $\Delta S_{r-t}$ , conformational, solvation, and roto-translational entropy changes, respectively;  $\Delta A$ , surface area change;  $\Delta c_{pi}$ , specific heat capacity for the surface area of the type i;  $\alpha$ , cooperative heterotropic association constant;  $\Delta h$ , cooperative enthalpy;  $\Delta s$ , cooperative entropy.

which, although catalytically inactive, bind nucleotides with considerable affinity (6–12).

According to the binding change mechanism (2), the three catalytic sites act in a concerted manner, alternating sequentially through three different conformations (tight, loose, and open) with vastly different substrate affinities [high (S1), medium (S2), and low (S3) affinity]. These sites exhibit strong positive and negative cooperativity in catalysis and binding, respectively (13). High-resolution crystal structures of  $F_1$  have yielded invaluable information for unveiling key molecular elements of the binding change mechanism (1, 14–22). The structure of bovine mitochondrial  $F_1$  bound to Mg·nucleotides (the Mg·ADP-inhibited  $F_1$  state) obtained by Abrahams et al. (1) revealed the three  $\beta$  subunits in different conformations. One  $\beta$  subunit ( $\beta_E$ ) shows an open conformation and has an empty catalytic site. The other two  $\beta$  subunits are in the closed conformation, one binding Mg·ADP ( $\beta_{DP}$ ) and the other binding Mg·AMPPNP ( $\beta_{TP}$ ). Noninhibited structures of bovine and yeast mitochondrial  $F_1$  have also been determined (20, 21). In these structures, the  $\beta_{DP}$  catalytic site is occupied by Mg·AMPPNP.

In spite of the impressive advances in establishing the molecular bases of the function of  $F_0F_1$ -ATP synthase and its different subcomplexes, many key aspects remain to be unveiled. In particular, knowledge of the energetic principles that drive substrate recognition and intersubunit communication is still rudimentary. The energetic contribution of Mg(II) in this enzyme is also poorly understood (2). Besides its role as a cofactor required for stabilization of the transition state (23), Mg(II) has been implicated as being crucial in determining the binding asymmetry and cooperativity between catalytic sites (24, 25). However, recent studies have challenged that conclusion, indicating that heterogeneity in  $\beta$  subunit affinities is an inherent property of nucleotide-free  $F_1$  (22, 26, 27). As far as we know, no systematic characterization of the energetic contribution of Mg(II) in the recognition of nucleotides by  $F_1$  or by the isolated subunits has been conducted.

Nucleotide-induced conformational changes in  $\beta$  subunits are considered to be the essential driving force for rotational catalysis in  $F_1$  (1, 3, 4, 11, 12, 28, 29). Saliiently, the isolated  $\beta$  subunit undergoes conformational changes that resemble those between open and closed  $\beta$  subunit conformations in  $F_1$  crystal structures (6, 7, 10–12, 30). Therefore, the isolated  $\beta$  subunit provides an excellent opportunity to study issues that are difficult to address in larger  $F_0F_1$ -ATP synthase subcomponents. In this work, we have aimed to gain new insights into the energetic bases of the recognition of adenosine nucleotides by the monomeric  $\beta$  subunit from thermophilic *Bacillus* PS3 ( $T\beta$ ). For this purpose, the binding of  $T\beta$  to ATP and Mg·ATP was characterized as a function of temperature using high-precision isothermal titration calorimetry. The association of Mg(II) with free ATP was also characterized calorimetrically. The binding data of these complexes allowed the determination of the energetic contribution of Mg(II) in the recognition of ATP by  $T\beta$ . A similar analysis was performed for ADP as the ligand, and the properties of the two nucleotide complexes were compared. Finally, the energetic effects of Mg(II) in  $F_1$  catalytic sites were explored using affinity constants available in the literature.

## MATERIALS AND METHODS

**Materials.** All chemicals, including ATP and ADP sodium salts, were from Sigma Chemical Co.

**Expression and Purification of the  $T\beta$  Subunit.** Monomeric  $T\beta$  was expressed in *Escherichia coli* strain DK 8 (8), which lacks the genes for  $F_1F_0$ , and purified to homogeneity as previously described (30).

All experiments were performed at pH 8.0 in a 0.05 M Tris-HCl buffer solution supplemented with 0.1 M NaCl to prevent protein aggregation. Purified  $T\beta$  was thoroughly dialyzed against the buffer solution prior to calorimetric measurements. After degassing, the protein concentration was determined spectrophotometrically, using an extinction coefficient of  $15360 \text{ M}^{-1} \text{ cm}^{-1}$  at 280 nm. For ADP and ATP, an extinction coefficient of  $15600 \text{ M}^{-1} \text{ cm}^{-1}$  at 259 nm was used. MgCl<sub>2</sub> and nucleotides (sodium salts) were dissolved into the buffer solution obtained from the last dialysis. The solution's pH was readjusted to 8.0 using NaOH when necessary.

**Isothermal Titration Calorimetry.** ITC determinations were performed using the high-precision VP-ITC microcalorimeter (MicroCal, Inc.). Binding of  $T\beta$  to Mg·ATP or ATP was assessed in the temperature range of 15–30 °C. The  $T\beta$  concentration was typically 0.05–0.07 mM, while the ligand concentration in the syringe was 2.0–2.5 mM. In the titration of  $T\beta$  with the Mg(II)-free nucleotide, ligand and protein solutions were supplemented with 2 mM EDTA to sequester any residual trace of Mg(II) in the solution. The titration schedule consisted of 20–30 consecutive injections of 3–8  $\mu\text{L}$  with a 6 min interval between injections. The dilution heat of the ligand was obtained via addition of the ligand to a buffer solution under identical conditions and the injection schedule used with the protein sample. In the case of the titration of  $T\beta$  with Mg(II)-free nucleotide, the binding constant ( $K_b$ ), the enthalpy change ( $\Delta H_b$ ), and the stoichiometry ( $n$ ) were determined by nonlinear fitting of normalized titration data using an identical and independent binding site model (31):

$$Q = \frac{nM_T \Delta H_b V_0}{2} \left[ 1 + \frac{X_T}{nM_T} + \frac{1}{nK_b M_T} \right. \\ \left. - \sqrt{\left( 1 + \frac{X_T}{nM_T} + \frac{1}{nK_b M_T} \right)^2 - \frac{4X_T}{nM_T}} \right]$$

where  $Q$  is the normalized differential heat evolved per mole of ligand, after correction for the heats of dilution of the ligand,  $V_0$  is the working volume of the cell, and  $X_T$  and  $M_T$  are the ligand and macromolecule concentrations, respectively. For the titration of  $T\beta$  with Mg(II)-bound ATP, both the ligand and protein solutions contained 5 mM MgCl<sub>2</sub>. The resulting binding isotherms were analyzed using a ternary model in which  $T\beta$  may bind ATP or Mg·ATP, while ATP may also be in the form of Mg<sub>2</sub>·ATP (see Appendix). In the fitting of this model, formation parameter values for  $T\beta$ ·ATP, Mg·ATP, and Mg<sub>2</sub>·ATP (determined in independent experiments) were kept fixed, while those for the  $T\beta$ –Mg·ATP complex were the fitting parameters.

Titration of ATP with MgCl<sub>2</sub> was performed in the temperature range of 15–30 °C. The reaction cell contained 1.5 mM ATP, and the syringe contained 80 mM MgCl<sub>2</sub>. Each titration consisted of a series of 35 consecutive injections of 2–15  $\mu\text{L}$  with a 10 min interval between injections. The binding isotherms were analyzed using a model in which two Mg(II) ions bind sequentially to ATP (32):

$$Q = ([\text{ATP}]_T V_0) \{ [K_{b1} [\text{Mg}] \Delta H_{b1} + K_{b1} K_{b2} [\text{Mg}]^2 (\Delta H_{b1} \\ + \Delta H_{b2})] / (1 + K_{b1} [\text{Mg}] + K_{b1} K_{b2} [\text{Mg}]^2) \}$$

where  $Q$  is the cumulative heat effect, subscripts 1 and 2 stand for the binding of the first and second Mg(II), respectively,  $[ATP]_T$  is the total ATP concentration, and  $[Mg]$  is the free Mg(II) concentration.

**Changes in Solvent-Accessible Surface Area.** Surface area calculations were conducted with NACCESS [Hubbard, S. J., and Thornton, J. M. (1993) *NACCESS*, Department of Biochemistry and Molecular Biology, University College, London], using a probe radius of 1.4 Å and a slice width of 0.1 Å. Changes in solvent-accessible surface areas ( $\Delta A$ ) were estimated from the difference between the complex and the sum of the free molecules.

**$\Delta A$ -Based Calculations of  $\Delta C_{pb}$ .** To estimate  $\Delta C_{pb}$  from structural data, we used the semiempirical relationship

$$\Delta C_{pb} = \sum \Delta c_{pi} \Delta A_i$$

where  $\Delta c_{pi}$  is the specific heat capacity contribution per unit of surface area of type  $i$ . Parameters for protein's apolar (carbon and sulfur atoms) and polar (oxygen and nitrogen atoms) surfaces, obtained from data of cyclic dipeptides for the transfer from the solid state to water, were taken from ref 33. These parameters were also used for the adenine surfaces. A recently published sugar-specific parametrization was used for the ribose moiety in the nucleotide (34). For Mg(II) and phosphate surfaces, we derived corresponding specific parameters. Heat capacity changes accompanying the transfer of magnesium and inorganic phosphate from the gas phase to an aqueous solution were taken from ref 35. These magnitudes ( $-41$  and  $-81$  cal mol<sup>-1</sup> K<sup>-1</sup> for magnesium and inorganic phosphate, respectively) were then corrected for expansion effects by adding to them  $R$ , the universal constant of ideal gases (36), and normalized by the corresponding total surface area (113 and 188 Å<sup>2</sup> for magnesium and inorganic phosphate, respectively).

## RESULTS

**Thermodynamics of Mg(II) Binding to Free ATP.** At pH 8, ATP is completely unprotonated (ATP<sup>4-</sup>). Therefore, it is able to bind two Mg(II) ions in a stepwise manner:



Consistent with this, binding isotherms obtained for the titration of ATP with MgCl<sub>2</sub> were best described with a sequential binding site model (Figure 1). Results from calorimetric measurements performed at different temperatures are summarized in Table 1. ATP binds the first Mg(II) with an ~400-fold avidity in relation to the second one. Both binding events are entropically driven, with the enthalpic component being more unfavorable for the formation of the mono-Mg(II) species. Assuming  $\Delta C_{pb}$  is temperature-independent, a linear regression analysis of  $\Delta H_b$  data versus temperature in Table 1 gives values of  $37 \pm 10$  and  $20 \pm 10$  cal mol<sup>-1</sup> K<sup>-1</sup> for Mg-ATP and Mg<sub>2</sub>-ATP complexes, respectively (Figure 2). The  $\Delta H_{b1}$  and  $K_{b1}$  values obtained here are similar to those recommended by Smith et al. (37) ( $T = 25$  °C,  $\Delta H_b = 4.49$  kcal mol<sup>-1</sup>, and  $K_b = 35500$  M<sup>-1</sup>), who compiled and critically examined a large set of published binding data for the Mg-ATP complex. As far as we know, only one ITC study of the interaction of Mg(II) with ATP has been reported (38). Data in that study (28 °C) were analyzed using a single-site model, yielding a similar enthalpy change ( $\Delta H_b = 4.2$  kcal/mol), but a somewhat smaller binding constant ( $K_b = 9600$  M<sup>-1</sup>) compared to those listed in Table 1. In contrast to the large number of  $\Delta H_b$

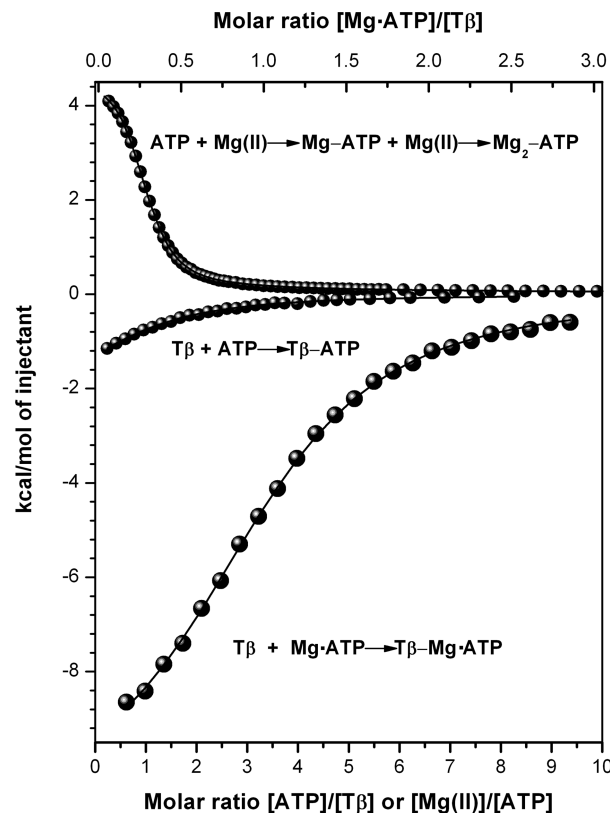


FIGURE 1: Calorimetric isotherms for the formation of T $\beta$ -ATP, T $\beta$ -Mg-ATP, Mg-ATP, and Mg<sub>2</sub>-ATP complexes at 25 °C, in a 0.05 M Tris-HCl buffer solution supplemented with 0.1 M NaCl (pH 8.0). Solid lines correspond to the best fitting curves. In the titration of ATP with Mg(II), the experimental data were best fitted with a sequential binding two-site model. For the T $\beta$ -ATP complex, an identical and independent binding site model was used. In the case of the T $\beta$ -Mg-ATP complex, a coupled equilibrium model was used which considers the binding of T $\beta$  to ATP or Mg-ATP and the binding of ATP to one or two magnesium ions.

and  $K_b$  values available in the literature,  $\Delta C_{pb}$  values are still scarce. Alberty (39) reported a value of 30 cal mol<sup>-1</sup> K<sup>-1</sup> for the Mg-ATP complex, which is similar to that obtained in this study. In contrast, Wang et al. (40), using isothermal flow calorimetric data in the temperature range of 50–125 °C, obtained significantly larger values for the two Mg(II)-bound ATP complexes (121 and 50 cal mol<sup>-1</sup> K<sup>-1</sup> for Mg-ATP and Mg<sub>2</sub>-ATP complexes, respectively).

**Thermodynamics of ATP and Mg-ATP Binding to Isolated T $\beta$ .** Figure 1 shows examples of binding isotherms obtained for T $\beta$ -ATP and T $\beta$ -Mg-ATP complexes.<sup>2</sup> The binding isotherms for the T $\beta$ -ATP complex were well fitted using a single-site binding model. For the titration of T $\beta$  with Mg(II)-bound ATP, the calorimetric data were fitted using a model in which ATP and Mg-ATP compete for T $\beta$ 's binding site, and the equilibria among the ATP, Mg-ATP, and Mg<sub>2</sub>-ATP species are taken into account (see Appendix).

Table 2 summarizes the calorimetric results obtained for T $\beta$ -ATP and T $\beta$ -Mg-ATP complexes at different temperatures. For both binding events, calorimetric data consistently yielded an ~1:1 stoichiometry. The two complexes differ significantly from each other in their thermodynamic properties.

<sup>2</sup>The new noncovalent bond formed in the considered binding reaction is indicated by a dash. In the formation of a ternary complex, the noncovalent contact in the preformed binary complex is indicated by a center dot.

Table 1: Thermodynamic Parameters for the Binding of Mg(II) to ATP at Different Temperatures<sup>a</sup>

temp (°C)	Mg-ATP				Mg <sub>2</sub> -ATP			
	$K_{b1}$ ( $\times 10^{-4} \text{ M}^{-1}$ )	$\Delta G_{b1}$ (kcal/mol)	$\Delta H_{b1}$ (kcal/mol)	$T\Delta S_{b1}$ (kcal/mol)	$K_{b2}$ ( $\text{M}^{-1}$ )	$\Delta G_{b2}$ (kcal/mol)	$\Delta H_{b2}$ (kcal/mol)	$T\Delta S_{b2}$ (kcal/mol)
15	2.2 ± 0.2	-5.7	3.9 ± 0.1	9.6	49 ± 21	-2.2	1.5 ± 0.2	3.7
20	3.0 ± 0.0	-6.0	4.2 ± 0.1	10.2	63 ± 7	-2.4	1.5 ± 0.1	3.9
25	3.6 ± 0.1	-6.2	4.4 ± 0.2	10.6	98 ± 15	-2.7	1.7 ± 0.2	4.4
30	4.0 ± 0.1	-6.4	4.6 ± 0.1	11.0	101 ± 17	-2.8	1.8 ± 0.1	4.6

<sup>a</sup>Equilibrium constants correspond to stepwise association constants. Values are means of three independent experiments at each temperature.

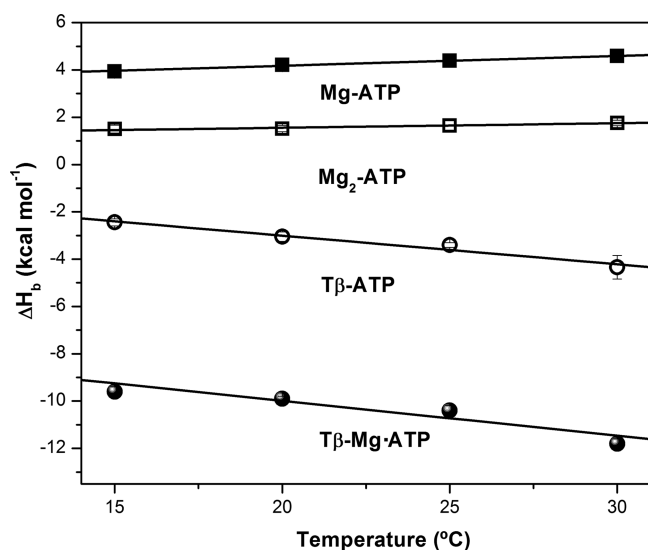


FIGURE 2: Binding enthalpies as a function of temperature for the Tβ-ATP, Tβ-Mg·ATP, Mg-ATP, and Mg<sub>2</sub>-ATP complexes in a 0.05 M Tris-HCl buffer solution supplemented with 0.1 M NaCl (pH 8.0). Dashed lines correspond to the least-squares linear fittings of the Kirchoff equation ( $\partial\Delta H_b/\partial T = \Delta C_p$ ) to the calorimetric data, assuming  $\Delta C_p$  is independent of temperature.

The 7-fold association constant value obtained for the Tβ-Mg·ATP complex arises from significant, although partially counterbalanced, variations in enthalpy and entropy. At all temperatures sampled, Tβ binding to Mg·ATP was around 2-fold more exothermic than that to ATP. In contrast, the binding entropy was more favorable for the Tβ-ATP complex.

Also using ITC, Odaka et al. (8) measured Tβ-Mg·ATP binding energetics at a single temperature (21 °C). Data obtained in that study ( $\Delta H_b = -12$  kcal/mol,  $T\Delta S_b = -5.5$  kcal/mol, and  $K_b = 66000 \text{ M}^{-1}$ ) are somewhat different from those in Table 2. These differences are in part due to the use of different binding models. In fact, if our binding isotherms were analyzed using a simple 1:1 binding model, values closer to those of Odaka et al. would be obtained (for instance, at 20 °C,  $\Delta H_b$  and  $T\Delta S_b$  would be  $-10.7$  and  $-4.1$  kcal/mol, respectively). These contrasting results illustrate the importance of taking into account the coupled equilibria occurring during the titration of Tβ with Mg(II)-bound ATP (i.e., that Tβ is able to bind Mg·ATP or ATP, and that ATP is able to bind one or two magnesium ions) for the determination of the true formation parameters of the Tβ-Mg·ATP complex. Analysis of the thermal dependence of  $\Delta H_b$  yields  $\Delta C_{pb}$  values of  $-150 \pm 20$  and  $-96 \pm 17 \text{ cal mol}^{-1} \text{ K}^{-1}$  for Tβ-Mg·ATP and Tβ-ATP complexes, respectively (Figure 2).

Table 3 shows the cooperativity parameters for the heterotropic interaction between magnesium and nucleotides. These

Table 2: Thermodynamic Parameters for the Binding of Mg·ATP or ATP to Tβ at Different Temperatures

temp (°C)	$K_b$ ( $\times 10^{-5} \text{ M}^{-1}$ )	$\Delta G_b$ (kcal/mol)	$\Delta H_b$ (kcal/mol)	$T\Delta S_b$ (kcal/mol)	$n$
Tβ-Mg·ATP					
15	1.8 ± 0.1	-6.9	-9.6 ± 0.2	-2.7	1.02 ± 0.01
20	1.3 ± 0.1	-6.9	-9.9 ± 0.1	-3.0	0.98 ± 0.01
25	1.0 ± 0.1	-6.8	-10.4 ± 0.2	-3.6	0.99 ± 0.01
30	0.73 ± 0.1	-6.7	-11.8 ± 0.2	-5.1	0.95 ± 0.02
Tβ-ATP					
15	0.25 ± 0.01	-5.8	-2.4 ± 0.2	3.4	0.98 ± 0.09
20	0.19 ± 0.00	-5.7	-3.1 ± 0.2	2.7	1.01 ± 0.05
25	0.13 ± 0.01	-5.6	-3.4 ± 0.1	2.2	1.05 ± 0.05
30	0.12 ± 0.01	-5.6	-4.3 ± 0.5	1.3	1.02 ± 0.10

Table 3: Thermodynamic Cooperativity Parameters for the Heterotropic Interaction in the Binding of Mg(II) and Nucleotides to Tβ at 25 °C

complex	$\alpha$	$\Delta g$ (kcal/mol)	$\Delta h$ (kcal/mol)	$T\Delta s$ (kcal/mol)
Tβ-Mg·ATP	7.7	-1.2	-7.0	-5.8
Tβ-Mg·ADP	1.1	-0.1	-3.4	-3.3

parameters, the cooperativity association constant,  $\alpha$ , and the cooperativity enthalpy,  $\Delta h$ , can be calculated from the thermodynamic parameters for the binding of the nucleotide and Mg-bound nucleotide to Tβ, and they reflect the reciprocal effect of each ligand on the binding to Tβ [ $\alpha = K_{P2}/K_{P1} = K_{b1}^*/K_{b1}$ , and  $\Delta h = \Delta H_{P2} - \Delta H_{P1} = \Delta H_{b1}^* - \Delta H_{b1}$  (see Appendix)].

## DISCUSSION

The elucidation of the molecular bases that govern the formation of noncovalent protein adducts requires a quantitative knowledge of the forces that drive the recognition process. In what follows, a structural-energetic analysis is presented for the formation of the Tβ complexes studied here, simultaneously considering the full set of thermodynamic functions.

*Tβ-Mg·ATP and Tβ-Mg·ADP Complexes Differ from Each Other Energetically and Structurally.* Figure 3 compares the thermodynamic signatures for the Tβ-Mg·ATP and Tβ-Mg·ADP complexes. For the last complex, the calorimetric data obtained previously (30) were fitted using the ternary binding model depicted in Appendix. For that purpose, the formation parameters of the Mg-ADP and Tβ-ADP complexes were also measured calorimetrically (see below). As seen in Figure 3, the presence of the  $\gamma$ -phosphate moiety makes the

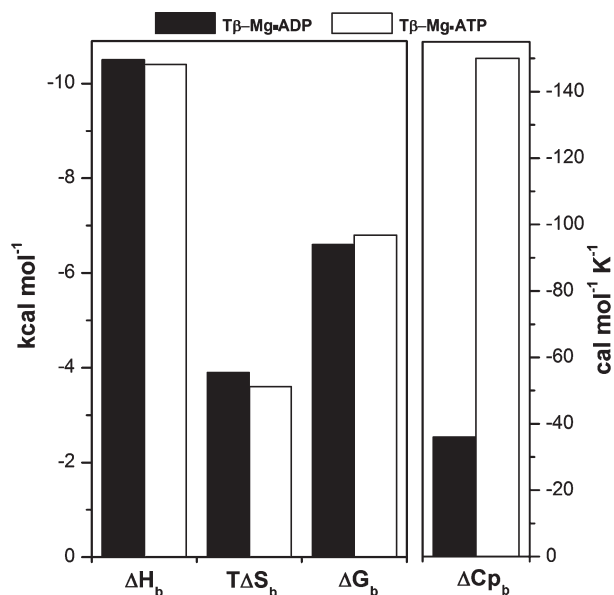


FIGURE 3: Thermodynamic signatures of Tβ-Mg-ATP and Tβ-Mg-ADP complexes at 25 °C as determined by isothermal titration calorimetry. See the legend of Figure 1 for the experimental conditions.

affinity slightly higher for Mg-ATP compared to that of Mg-ADP, with a binding enthalpy similar to that of Mg-ADP ( $\Delta\Delta H_b = -0.1$  kcal/mol), while the binding entropy becomes slightly less unfavorable [ $\Delta(T\Delta S_b) = 0.3$  kcal/mol]. In contrast, TF<sub>1</sub> catalytic sites exhibit a slightly stronger preference for Mg-ADP over Mg-ATP, indicating the importance of the oligomeric environment for substrate recognition (41). This preference is even more dramatic in the whole F<sub>0</sub>F<sub>1</sub>-ATP synthase, where the presence of the transmembrane proton gradient decreases the affinity for Mg-ATP by more than 6 orders of magnitude (42).

Figure 3 also compares  $\Delta C_{p,b}$  values for Tβ-Mg-ADP and Tβ-Mg-ATP complexes. The binding of Mg-ATP to Tβ elicits a significantly larger decrease in heat capacity in relation to Mg-ADP. Although exceptions can be found (34), typically the desolvation of polar surfaces increases the heat capacity, due to the liberation of water molecules that undergo a net gain of soft vibration modes upon return to the bulk solvent (43). In the case of phosphate groups, gas-to-water transfer data indicate that their desolvation yields positive heat capacity changes (35), which is consistent with the calorimetric results for the Mg-ATP and Mg<sub>2</sub>-ATP complexes (Figure 2). Thus, the more negative  $\Delta C_{p,b}$  value observed for the Tβ-Mg-ATP complex cannot be explained on the basis of γ-phosphate desolvation, suggesting the occurrence of additional molecular events.

Besides desolvation effects, a number of factors can contribute significantly to the heat capacity of biomolecular complexes, namely, (1) (de)protonation effects, (2) exchange of counterions, (3) sequestration or liberation of structural water molecules, and (4) conformational changes (43–45). For the Tβ-Mg-ADP complex, very similar binding values were obtained using Tris or cacodylate buffers (30). These buffers differ from each other largely in their ionization enthalpies ( $\Delta\Delta H_{ion} = 12$  kcal/mol) and in the electrical charge of their unprotonated bases (neutral for Tris and negative for cacodylate). Therefore, it seems that factors 1 and 2 can be ruled out as major contributors to  $\Delta C_{p,b}$  in the formation of Tβ-nucleotide complexes. On the other hand, scrutiny of the inhibited-state MF<sub>1</sub> structure (Protein Data Bank

Table 4: Surface Area Changes and Structure-Based Estimations of  $\Delta C_{p,b}$  for the Formation of Tβ-Mg-ADP and Tβ-Mg-ATP Complexes<sup>a</sup>

surface	$\Delta A$ (Å <sup>2</sup> )		$\Delta C_{pi}$ (cal mol <sup>-1</sup> K <sup>-1</sup> Å <sup>-2</sup> )
	Tβ-Mg-ADP	Tβ-Mg-ATP	
protein			
polar	-9	-61	-0.27 <sup>b</sup>
apolar	-240	-384	0.45 <sup>b</sup>
nucleotide			
magnesium	-72	-59	-0.36 <sup>c</sup>
phosphate	-143	-203	-0.43 <sup>c</sup>
hydroxyl (ribose)	-34	-39	0.10 <sup>d</sup>
no-ring carbon (ribose)	-19	-15	0.36 <sup>d</sup>
ring carbon (ribose)	-32	-29	0.09 <sup>d</sup>
nitrogen (adenine)	-107	-106	-0.27 <sup>b</sup>
carbon (adenine)	-84	-80	0.45 <sup>b</sup>
$\Delta A$ -based calculation			
$\Delta C_{p,calc}$ (cal mol <sup>-1</sup> K <sup>-1</sup> )	-40	-67	
$\Delta C_{p,exp}$ (cal mol <sup>-1</sup> K <sup>-1</sup> )	-36	-150	

<sup>a</sup>The atomic coordinates of the three β subunits were extracted from the X-ray structure of MF<sub>1</sub> [Protein Data Bank entry 1bmf (1)] and used to calculate  $\Delta A$  values for the binding of the isolated free β subunit (β<sub>E</sub>) to Mg-ADP (β<sub>DP</sub>) and Mg-ATP (β<sub>TP</sub>). <sup>b</sup>From ref 33. <sup>c</sup>Obtained from hydration heat capacities reported in ref 35. <sup>d</sup>From ref 34.

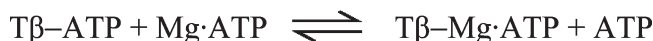
entry 1bmf) indicates that the two catalytic sites in closed conformation share similar residual hydration. Six and five water molecules are seen at the β<sub>DP</sub> and β<sub>TP</sub> sites, respectively, bridging the contact between the protein and the Mg-bound nucleotide ( $\leq 3.5$  Å cutoff). Thus, it seems that residual hydration effects (factor 3) are also not significant in the determination of the difference in  $\Delta C_{p,b}$  between Tβ-Mg-ADP and Tβ-Mg-ATP complexes.

A previous structural-energetic analysis showed that the small  $\Delta C_{p,b}$  ( $-36$  cal mol<sup>-1</sup> K<sup>-1</sup>) observed for the Tβ-Mg-ADP complex can be explained satisfactorily on the basis of desolvation of the protein binding site and ligand surfaces (30). In that analysis, the coordinates of the empty and the Mg-ADP-filled β subunits, extracted from the X-ray structure of inhibited MF<sub>1</sub> (1), were used for calculation of the changes in solvent accessibility of surface areas ( $\Delta A$ ) accompanying the formation of the complex. The large structural rearrangement involved in the transition from β<sub>E</sub> to β<sub>DP</sub> elicits extensive exposition and burying of surface areas at opposite zones of the protein. This strong compensatory effect yields a marginal net protein  $\Delta A$ , explaining why a small  $\Delta C_{p,b}$  value is observed experimentally. Following the same approach, area changes were calculated for the binding of Mg-ATP to the isolated β subunit, using the isolated structures of MF<sub>1</sub>'s β<sub>E</sub> and β<sub>TP</sub>. Table 4 lists  $\Delta A$  values for this complex and compares them with those for the Mg-ADP-bound complex. For this analysis, recently published sugar-specific parameters were used for ribose surfaces in the nucleotides (34). Furthermore, we derived specific heat capacity parameters for Mg(II) and phosphate surfaces, by using hydration data available in the literature (35). As shown in Table 4, the use of this refined set of parameters yields an excellent estimation of  $\Delta C_{p,b}$  for the Tβ-Mg-ADP complex. In contrast, in the case of the Tβ-Mg-ATP complex, the estimated value is approximately half of that measured calorimetrically, suggesting that the MF<sub>1</sub>'s β<sub>TP</sub> conformation is not as a good model as MF<sub>1</sub>'s β<sub>DP</sub> for the corresponding nucleotide-bound conformation of isolated Tβ.

Yagi et al. (10) measured the influence of nucleotides on the NMR signals of the 12 T $\beta$  tyrosine residues. The NMR spectra for T $\beta$  bound to ADP, Mg·ADP, and ATP were very similar to each other, while the T $\beta$ -Mg·ATP complex exhibited a dissimilar spectrum. More recently, Yagi et al. (12) performed a more detailed NMR analysis of the nucleotide-induced conformational changes in T $\beta$ . By using segmental isotope labeling, they found that the relative orientation of the C-terminal domain in Mg·ATP-bound and Mg·ADP-bound T $\beta$  complexes differs by 10°. These studies indicate that the monomeric T $\beta$  subunit adopts a closer conformation when bound to Mg·ATP. Thus, the more negative  $\Delta C_{pb}$  value of the T $\beta$ -Mg·ATP complex might be explained on the basis of a greater burial of protein surface area, elicited by a larger conformational change compared to that observed in MF<sub>1</sub>'s  $\beta_{TP}$  (1).

*Energetic Effects of Mg(II) in the Recognition of Nucleotides by Isolated T $\beta$ .* According to Hess' law, the difference between T $\beta$ -Mg·ATP and T $\beta$ -ATP complexes corresponds to the transfer of Mg(II) from ATP to the T $\beta$ ·ATP preformed complex:

Scheme 1



To determine the "pure" Mg(II) binding contribution



the association between the metal ion and free ATP needs to be taken into account:

Scheme 2

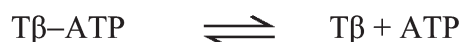


Table 5A shows calculations according to Scheme 2 using the thermodynamic data in Tables 1 and 2. Mg(II) binding is favored by ~7 kcal/mol of Gibbs free energy, versus the ~1 kcal/mol obtained from the difference between T $\beta$ -Mg·ATP and T $\beta$ -ATP complexes. Mg(II) sequestration by the T $\beta$ ·ATP complex is both enthalpically and entropically driven. In contrast, the straight difference between T $\beta$ -Mg·ATP and T $\beta$ -ATP complexes would lead to a different picture, i.e., that Mg(II) binding is enthalpically driven and entropically unfavored. The same results as those calculated considering Scheme 2 are obtained if the parameters for Mg(II) binding to the T $\beta$ -nucleotide complex are calculated using the binding parameters for Mg(II) binding to ATP and the cooperativity parameters [ $K_{b1}^* = \alpha K_{b1}$ , and  $\Delta H_{b1}^* = \Delta H_{b1} + \Delta h$  (see Appendix)]. In fact, this is another way of applying Hess' law.

To explore the molecular features of the incorporation of Mg(II) into the T $\beta$ ·ATP adduct, the theoretical  $\Delta C_{pb}$  was calculated for this binding event. In the structure of  $\beta_{TP}$  bound to Mg·AMPPNP extracted from the inhibited MF<sub>1</sub> crystal structure, the Mg(II) atom is completely inaccessible to the solvent. Removing Mg(II) from the complex yields virtually no surface area changes (<1 Å<sup>2</sup>) in either the nucleotide or the protein. Thus, in the case of a rigid body-like association between Mg(II) and T $\beta$ ·ATP, the heat capacity effect would correspond entirely to desolvation of the Mg(II) ion. The complete desolvation of an Mg(II) ion elicits a heat capacity increase of 39 cal mol<sup>-1</sup> K<sup>-1</sup>, once corrected for expansion effects (36). This value is significantly different from the negative  $\Delta C_{pb}$  value obtained from calorimetric data for the sequestration of Mg(II) by T $\beta$ ·ATP (Table 5A). Overall, these results indicate that some conformational rearrangements occur in the T $\beta$ ·ATP complex upon Mg(II) binding. This picture is consistent with the conformational variations between T $\beta$ ·ATP and T $\beta$ -Mg·ATP complexes evidenced from NMR data (10, 12).

The Mg(II) contribution in the T $\beta$ -Mg·ADP complex was also determined in this work. For that purpose, the formation parameters of the T $\beta$ -ADP and Mg-ADP complexes were measured calorimetrically (Table 5B). Similar to that observed with the Mg-ATP complex, binding of Mg(II) to free ADP is entropically driven and enthalpically unfavored, although with a binding constant that is 1 order of magnitude smaller ( $K_b = 2455 \pm 108$  M<sup>-1</sup>). In the case of the T $\beta$ -ADP complex, the interaction is both more stable ( $K_b = 60000$  M<sup>-1</sup>) and more exothermic (~2-fold more

Table 5: Thermodynamic Parameters for the Binding of Mg(II)<sup>a</sup>

(A) T $\beta$ ·ATP				
	$\Delta G_b$ (kcal/mol)	$\Delta H_b$ (kcal/mol)	$T\Delta S_b$ (kcal/mol)	$\Delta C_{pb}$ (cal mol <sup>-1</sup> K <sup>-1</sup> )
$T\beta + Mg \cdot ATP \rightleftharpoons T\beta - Mg \cdot ATP$	-6.8	-10.4	-3.6	-150
$T\beta - ATP \rightleftharpoons T\beta + ATP$	5.6	3.4	-2.2	99
$Mg(II) + ATP \rightleftharpoons Mg - ATP$	-6.2	4.4	10.6	37
$T\beta \cdot ATP + Mg(II) \rightleftharpoons T\beta - Mg \cdot ATP$	-7.4	-2.6	4.8	-14
(B) T $\beta$ ·ADP				
	$\Delta G_b$ (kcal/mol)	$\Delta H_b$ (kcal/mol)	$T\Delta S_b$ (kcal/mol)	
$T\beta + Mg \cdot ADP \rightleftharpoons T\beta - Mg \cdot ADP$	-6.6	-10.5	-3.9	
$T\beta \cdot ADP \rightleftharpoons T\beta + ADP$	6.5	7.1	0.6	
$Mg(II) + ADP \rightleftharpoons Mg - ADP$	-4.6	3.7	8.3	
$T\beta \cdot ADP + Mg(II) \rightleftharpoons T\beta - Mg \cdot ADP$	-4.7	0.3	5.0	

<sup>a</sup>All data obtained at 25 °C.

negative) than that of the  $T\beta$ -ATP complex. With the  $T\beta$ -ADP and  $Mg$ -ADP complex formation parameters determined, the calorimetric data reported previously for the  $T\beta$ - $Mg$ -ADP complex (30) were reanalyzed using the ternary model described in Appendix (Table 2). Since there was no evidence of the formation of the  $Mg_2$ -ADP complex,  $K_{b2}$  and  $\Delta H_{b2}$  were set to zero in the fitting analysis.

As shown in Table 5B, there are some differences in the binding energetics of the two nucleotides to  $T\beta$ . The interaction of  $T\beta$  with  $Mg$ -ATP is energetically similar to that of  $Mg$ -ADP. However, the thermodynamic differences between the  $T\beta$ - $Mg$ -ATP and  $T\beta$ -ATP complexes are significantly larger than those between the corresponding ADP complexes, indicating a very different effect of the metal ion in both types of nucleotide- $T\beta$  complexes. According to Scheme 2, the  $T\beta$ -ATP complex binds to  $Mg(II)$  with significantly more avidity. This improved affinity is mainly due to a favorable enthalpic contribution, while the binding entropies of both complexes are approximately the same size. The binding enthalpy is a measure of the strength of the interaction between the molecular partners ( $\Delta H_{int}$ ) relative to the energy penalty paid by desolvation ( $\Delta H_{dsolv}$ ) of the contact surfaces:

$$\Delta H_b = \Delta H_{int} + \Delta H_{dsolv}$$

Examples can be found in the literature of exothermic ( $\Delta H_{int} < -\Delta H_{dsolv}$ ) or exothermic ( $\Delta H_{int} > -\Delta H_{dsolv}$ ) recognition of metal ions by proteins (46). Accordingly, it is clear that the  $T\beta$ -ATP adduct provides a better stereochemical environment for  $Mg(II)$  anchoring than the  $T\beta$ -ADP adduct. In fact, mutational studies have shown that the complete octahedral coordination of  $Mg(II)$  in  $F_1$  closed catalytic sites requires the presence of the  $\gamma$ -phosphate of ATP (24). The  $\beta$ -phosphate of ATP and four  $\beta$  subunit residues (three of them linked via structural water molecules) complement the coordination of the metal ion. Furthermore, since no  $\alpha$  subunit residue is involved in the binding to  $Mg(II)$  in  $F_1$ , in principle the full coordination of the metal ion can be achieved in the isolated  $\beta$  subunit.

Another way to look at the effect of  $Mg(II)$  in the recognition of nucleotides by  $T\beta$  is through the cooperative heterotropic association constant ( $\alpha$ ), which is calculated as the ratio between the  $T\beta$ - $Mg$ -ATP and  $T\beta$ -ATP binding constants (see Appendix) (47, 48). According to the data listed in Table 3, the binding of ATP and  $Mg(II)$  to  $T\beta$  is highly cooperative ( $\alpha = 7.7$ ), while  $Mg(II)$  has virtually no effect in the case of ADP ( $\alpha = 1.1$ ). Similarly, the cooperative enthalpy ( $\Delta h$ ) is given by the enthalpy difference between the  $Mg(II)$ -bound and  $Mg(II)$ -free nucleotide- $T\beta$  complexes. For ATP recognition,  $\Delta h$  is  $-7.0$  kcal/mol, whereas for ADP,  $\Delta h$  is  $-3.4$  kcal/mol. The cooperative entropic term for ATP ( $\Delta s$ ) is  $-5.8$  cal mol $^{-1}$  K $^{-1}$ , whereas for ADP it is  $-3.3$  cal mol $^{-1}$  K $^{-1}$ . In the case of ADP, the cooperative enthalpy and entropy cancel out, giving rise to a negligible cooperative Gibbs energy. Besides, both enthalpic and entropic terms for ATP are smaller (approximately 2-fold) than those for ADP. With regard to the binding cooperativity in the  $T\beta$ - $Mg$ -ADP ternary system, from a formal point of view it is interesting to point out that, considering ATP as the reference binding molecule, this system represents an example of coupling between a cooperative homotropic interaction [ATP may bind one or two  $Mg(II)$  ions] and cooperative heterotropic interaction [ATP may bind  $T\beta$ , may bind  $Mg(II)$ , or may bind both  $T\beta$  and

$Mg(II)$  simultaneously, but the binding of a second  $Mg(II)$  excludes the binding of ATP].

It is interesting to note that while the difference in the enthalpy of formation between  $T\beta$ - $Mg$ -ATP and  $T\beta$ - $Mg$ -ADP ( $\Delta\Delta H_b = -0.1$  kcal/mol) complexes is very similar to that between  $Mg$ -ATP and  $Mg$ -ADP complexes ( $\Delta\Delta H_b = -0.3$  kcal/mol), the difference in the entropy of formation between the protein adducts is significantly smaller [ $\Delta(T\Delta S_b)$  of 0.3 kcal/mol vs  $\Delta(T\Delta S_b)$  of 2.3 kcal/mol] (Table 5B). The net change in the number of degrees of freedom upon molecular association is determined by three major contributions, namely

$$\Delta S_b = \Delta S_{conf} + \Delta S_{solv} + \Delta S_{r-t}$$

where  $\Delta S_{conf}$ ,  $\Delta S_{solv}$ , and  $\Delta S_{r-t}$  stand for the conformational, solvation, and roto-translational entropy changes, respectively (33). It is well established that the formation of bimolecular complexes involves a constant loss of  $\Delta S_{r-t}$ , regardless of the size of the interacting molecules (49). On the other hand, the presence of the  $\gamma$ -phosphate of ATP should yield a more favorable  $\Delta S_{solv}$ , since a larger surface area becomes buried upon binding to the protein. Therefore, the smaller entropy difference between  $T\beta$ - $Mg$ -ATP and  $T\beta$ - $Mg$ -ADP complexes in relation to that between  $Mg$ -ATP and  $Mg$ -ADP complexes may be interpreted in terms of a more unfavorable  $\Delta S_{conf}$  for the formation of the  $T\beta$ - $Mg$ -ATP complex, i.e., the freezing of a larger number of protein rotatable bonds.

Overall, the analysis given above indicates that the  $T\beta$ -ATP adduct provides a better site for  $Mg(II)$  anchoring than the  $T\beta$ -ADP adduct. Furthermore, entropy and heat capacity changes are consistent with the catalytic subunit adopting a more closed conformation when it is bound to  $Mg$ -ATP than when it is bound to ATP or  $Mg$ -ADP. These results confirm and complement in energetic terms the conclusions reached recently by Yagi et al. (12), who found that in the presence of  $Mg(II)$ , the  $\gamma$ -phosphate elicits a structural rearrangement at the catalytic site that follows the overall bending motion, a rearrangement that is not seen upon ADP or  $Mg$ -ADP binding.

*Energetic Role of Mg(II) in the Recognition of ATP by Catalytic Sites in F<sub>1</sub>.* In spite of the wealth of available information about the catalytic and binding properties of  $F_1$ , there is still a debate regarding whether the occupancy of two (2, 26, 27, 50) or three catalytic sites (41, 51, 52) is sufficient to achieve rapid ATPase activity. Furthermore, binding and kinetic data of ATP synthase and its different subcomplexes have proven to be difficult to analyze and interpret. For instance, although  $F_1$  catalytic sites exhibit strong negative binding cooperativity (13, 53), experimental data have been just as well-described using sequential or independent site models (26, 41). Needless to say, settlement of these mechanistic aspects is essential for the correct determination of  $F_1$  binding parameters. Studies based on either bi- or tri-site models have been conducted for measurement of the association constants of both  $Mg(II)$ -free and  $Mg(II)$ -bound nucleotides. Thus, just as with the isolated  $T\beta$  subunit, the Gibbs free energy contributions of  $Mg(II)$  in  $F_1$  catalytic sites were determined using both bi- and tri-site binding data. It is worth recalling that, according to the analysis presented above for isolated  $T\beta$ , the determination of the true thermodynamic parameters for the recognition of the  $Mg(II)$ -bound nucleotide requires the simultaneous consideration of the association parameters of the free nucleotide with  $T\beta$

Table 6: Binding Energetics of F<sub>1</sub> Catalytic Sites<sup>a</sup>

(A) Tri-site Data for EF <sub>1</sub> <sup>b</sup>							
$\Delta G_b(S1)$	$\Delta G_b(S2)$	$\Delta G_b(S3)$	$\Delta G_b(S1) = \Delta G_b(S2) = \Delta G_b(S3)$	$\Delta G_b(S1)$	$\Delta G_b(S2)$	$\Delta G_b(S3)$	ref
-10.43	EF <sub>1</sub> $\beta$ + Mg·ATP -7.93	-6.17	EF <sub>1</sub> $\beta$ + ATP -5.79	-10.84	EF <sub>1</sub> $\beta$ ·ATP + Mg(II) -8.36	-6.50	54
-10.02	EF <sub>1</sub> $\beta$ + Mg·ADP -7.78	-6.04	EF <sub>1</sub> $\beta$ + ADP -5.53	-10.29	EF <sub>1</sub> $\beta$ ·ADP + Mg(II) -8.05	-5.80	54
(B) Bi-site Data for EF <sub>1</sub> <sup>b</sup>							
$\Delta G_b(S1)$	$\Delta G_b(S2)$	$\Delta G_b(S1)$	$\Delta G_b(S2)$	$\Delta G_b(S1)$	$\Delta G_b(S2)$		ref
-10.80	EF <sub>1</sub> $\beta$ + Mg·ADP -6.88	-9.95	EF <sub>1</sub> $\beta$ + ADP -5.99	-6.91	EF <sub>1</sub> $\beta$ ·ADP + Mg(II) -6.95		27
(C) Tri-site Data for TF <sub>1</sub> <sup>c</sup>							
$\Delta G_b(S2)$	$\Delta G_b(S3)$	$\Delta G_b(S2)$	$\Delta G_b(S3)$	$\Delta G_b(S2)$	$\Delta G_b(S3)$		ref
-9.00	TF <sub>1</sub> $\beta$ + Mg·ATP -6.26	-6.91	TF <sub>1</sub> $\beta$ + ATP -5.60	-8.28	TF <sub>1</sub> $\beta$ ·ATP + Mg(II) -6.71		35, 55
-9.11	TF <sub>1</sub> $\beta$ + Mg·ADP -6.37	-7.85	TF <sub>1</sub> $\beta$ + ADP -6.19	-5.88	TF <sub>1</sub> $\beta$ ·ADP + Mg(II) -4.80		35, 55

<sup>a</sup> $\Delta G_b$  values are given in kilocalories per mole. <sup>b</sup>Data obtained at 23 °C. <sup>c</sup>Data obtained at 25 °C.

or Mg(II). Nevertheless, in the case of T $\beta$ , the consideration of all the different coupled equilibria simultaneously yields only minor differences in the  $\Delta H_b$  and  $\Delta S_b$  values (<2 kcal/mol) determined using either a simple binary binding model or a complex ternary model, while the differences in  $\Delta G_b$  were negligible (<0.2 kcal/mol).

Senior and colleagues have thoroughly studied F<sub>1</sub> from *E. coli* (EF<sub>1</sub>) following the quenching of a Trp residue introduced at position 331 in the  $\beta$  subunit (EF<sub>1</sub> $\beta$ Y331W) (24, 25, 42, 51, 54). Binding data were analyzed using a model of three independent sites (S1–S3). Table 6A shows Gibbs free energies for the binding of EF<sub>1</sub> catalytic sites to ADP and ATP, in the presence or absence of Mg(II). In the presence of the metal ion, three different affinities were observed. According to these data, EF<sub>1</sub> exhibits a somewhat stronger avidity for Mg·ATP than for Mg·ADP. For both nucleotides,  $\Delta G_b(S1)$  is ~2.5 kcal/mol more exergonic than  $\Delta G_b(S2)$ , which in turn is ~1.7 kcal/mol more negative than  $\Delta G_b(S3)$ . In contrast, the three sites exhibited identical affinities in the absence of Mg(II). This last result led to the proposal that Mg(II) is essential for imparting asymmetric binding properties in F<sub>1</sub>.

In a recent study, Bulygin and Milgrom (27) noted that sulfate competes with adenosine nucleotides for catalytic sites in EF<sub>1</sub>, similar to that observed previously for inorganic phosphate. This observation is relevant, as a large body of data (including those from Senior's lab) has been obtained with sulfate as a cosolute. Bulygin and Milgrom (27) obtained binding constants of sulfate-free EF<sub>1</sub> $\beta$ Y331W for ADP, Mg·ADP, and ATP considering two independent binding sites, while Mg·ATP was not measured in that study. Therefore, Table 6B lists only bi-site binding data for ADP and Mg·ADP. Measurements performed in the absence of sulfate revealed that EF<sub>1</sub> $\beta$ Y331W catalytic sites also exhibit different affinities for Mg(II)-free nucleotides, an observation that contradicts the view that the metal ion is the determinant for the nucleotide binding asymmetry. For Mg·ADP, the difference between  $\Delta G_b(S1)$  and  $\Delta G_b(S2)$  (~4 kcal/mol) is significantly larger than the difference between the same two sites in the tri-site model (~2.5 kcal/mol). Furthermore, in the bi-site model, the

difference in affinity between S1 and S2 is not sensitive to the presence or absence of Mg(II).

Allison and co-workers reported tri-site binding data for TF<sub>1</sub> also using mutant  $\beta$  subunits,  $\beta$ Y341W (41, 55). Table 6C lists values for only catalytic sites S2 and S3, since under the conditions used by the authors, only the upper limits for  $\Delta G_b(S1)$  were inferred.  $\Delta G_b(S2)$  values for Mg(II)-bound nucleotides are significantly more exergonic for TF<sub>1</sub> than for EF<sub>1</sub>, while  $\Delta G_b(S3)$  values are rather similar. For the binding of Mg(II)-free nucleotides, three different affinities were observed for TF<sub>1</sub>, with  $\Delta G_b(S3)$  being comparable to the single affinity value obtained for the three EF<sub>1</sub> catalytic sites.

Bi- or tri-site binding models lead to very different pictures of the role of Mg(II) in stabilization in F<sub>1</sub> (Table 5). Data inferred from the tri-site model indicate that incorporation of the Mg(II) ion depends strongly on the conformation of the catalytic site, with the strength of the stabilization paralleling the affinity for the Mg(II)-bound nucleotide. This conclusion remains the same, regardless of whether the three catalytic sites are thought to have different or identical affinities for Mg(II)-depleted nucleotides. In the case of EF<sub>1</sub>, the difference between  $\Delta G_b(S1)$  and  $\Delta G_b(S2)$  is larger than that between  $\Delta G_b(S2)$  and  $\Delta G_b(S3)$ . Since  $\beta_{TP}$  and  $\beta_{DP}$  are conformationally very similar to each other, it follows that Mg(II) perceives in some way the asymmetric environment provided by the adjacent  $\alpha$  and  $\gamma$  subunits. In contrast, the bi-site model leads to the conclusion that Mg(II) contributes similarly in both catalytic sites. In other words, Mg(II) does not make any contribution per se to the heterogeneity of the catalytic sites, at least in terms of  $\Delta G_b$ . The idea that intersubunit interactions alone induce nucleotide binding heterogeneity at catalytic sites has recently received important support from the recently determined crystal structure of nucleotide-free mitochondrial F<sub>1</sub>, where the three  $\beta$  subunits present different conformations (22), as in the structure of nucleotide-bound MF<sub>1</sub>.

Like those observed for isolated T $\beta$ , available affinity constants for F<sub>1</sub> catalytic sites indicate that the stabilization effects of Mg(II) depend significantly on the nucleotide

involved. Furthermore, it has recently been suggested that to liberate products efficiently, the ADP-releasing  $\beta$  subunit in  $F_1$  should adopt a less closed conformation compared to that of the ATP-bound subunit (12). Thus, the nucleotide-dependent conformational and energetic behavior of the monomeric subunit seems to have functional repercussions in  $F_1$ . To further explore the energetic bases that drive nucleotide recognition by  $F_1$  catalytic sites, a calorimetric characterization of the binding of this oligomer to Mg(II)-free and Mg(II)-bound nucleotides is currently being undertaken in our lab.

### ACKNOWLEDGMENT

We thank M. in S. Virginia Gómez Vidales for her invaluable assistance in the ITC experiments and Drs. Armando Gómez-Puyou and Marietta Tuena de Gómez-Puyou (IFC, UNAM) for their critical reading of the manuscript prior to its submission.

### APPENDIX

We will consider a ternary system in which the  $T\beta$  subunit may bind ATP or  $Mg \cdot ATP$  and, at the same time, ATP may bind one or two magnesium ions (Scheme 3).

The concentration of the different complexes can be expressed as a function of the concentrations of free species:

$$\begin{aligned} [Mg \cdot ATP] &= K_{b1}[ATP][Mg(II)] \\ [Mg_2 \cdot ATP] &= K_{b1}K_{b2}[ATP][Mg(II)]^2 \\ [T\beta \cdot ATP] &= K_{p1}[T\beta][ATP] \\ [T\beta \cdot Mg \cdot ATP] &= K_{p2}K_{b1}[T\beta][ATP][Mg(II)] = \\ &K_{p1}K_{b1} * [T\beta][ATP][Mg(II)] \end{aligned}$$

Considering the mass conservation for each component [ $T\beta$ , ATP, and  $Mg(II)$ ]:

$$\begin{aligned} [ATP]_T &= [ATP] + [Mg \cdot ATP] + [Mg_2 \cdot ATP] + [T\beta \cdot ATP] \\ &\quad + [T\beta \cdot Mg \cdot ATP] \\ [Mg]_T &= [Mg(II)] + [Mg \cdot ATP] + 2[Mg_2 \cdot ATP] \\ &\quad + [T\beta \cdot Mg \cdot ATP] \\ [T\beta]_T &= [T\beta] + [T\beta \cdot ATP] + [T\beta \cdot Mg \cdot ATP] \end{aligned}$$

Then, introducing the equilibrium constants for each complex, we arrive at the following set of nonlinear equations:

$$\begin{aligned} [ATP]_T &= [ATP] + K_{b1}[ATP][Mg(II)] + K_{b1}K_{b2}[ATP][Mg(II)]^2 \\ &\quad + K_{p1}[T\beta][ATP] + K_{p2}K_{b1}[T\beta][ATP][Mg(II)] \\ [Mg]_T &= [Mg(II)] + K_{b1}[ATP][Mg(II)] + 2K_{b1}K_{b2}[ATP][Mg(II)]^2 \\ &\quad + K_{p2}K_{b1}[T\beta][ATP][Mg(II)] \\ [T\beta]_T &= [T\beta] + K_{p1}[T\beta][ATP] + K_{p2}K_{b1}[T\beta][ATP][Mg(II)] \end{aligned}$$

where  $K_{b1}$  and  $K_{b2}$  are the stepwise association constants for the sequential binding of  $Mg(II)$  to ATP,  $K_{p1}$  and  $K_{p2}$  are the

association constants for ATP and  $Mg \cdot ATP$  binding to  $T\beta$ , respectively, and  $K_{b1}^*$  is the association constant for  $Mg(II)$  binding to  $T\beta \cdot ATP$ .

The total concentrations of ATP, magnesium, and  $T\beta$  after each calorimetric injection  $i$  are given by

$$\begin{aligned} [ATP]_{T,i} &= [ATP]_0 \left[ 1 - \left( 1 - \frac{v}{V_0} \right)^i \right] \\ [Mg]_{T,i} &= [Mg]_0 \\ [T\beta]_{T,i} &= [T\beta]_0 \left( 1 - \frac{v}{V_0} \right)^i \end{aligned}$$

where  $[ATP]_0$  is the concentration of ATP in the syringe,  $[Mg]_0$  is the concentration of magnesium in the syringe and the cell,  $[T\beta]_0$  is the initial concentration of  $T\beta$  in the cell,  $v$  is the injection volume, and  $V_0$  is the cell volume.

The Newton–Raphson method can be used to solve numerically the set of nonlinear equations for each titration point, thus, determining the free concentrations of ATP, magnesium, and  $T\beta$  after each calorimetric injection. Using the association constants, the concentration of each complex after each injection can be calculated:

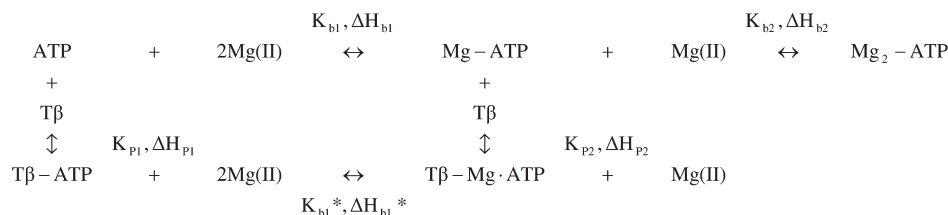
$$\begin{aligned} [T\beta \cdot ATP]_i &= K_{p1}[T\beta]_i[ATP]_i \\ [T\beta \cdot Mg \cdot ATP]_i &= K_{p2}K_{b1}[T\beta]_i[ATP]_i[Mg]_i \\ [Mg \cdot ATP]_i &= K_{b1}[ATP]_i[Mg]_i \\ [Mg_2 \cdot ATP]_i &= K_{b1}K_{b2}[ATP]_i[Mg]_i^2 \end{aligned}$$

The heat effect associated with each injection,  $q_i$ , can be calculated from the change in concentration for each complex after each calorimetric injection, and the enthalpy change associated with formation of each complex:

$$\begin{aligned} q_i &= V_0 \left\{ \left[ [T\beta \cdot ATP]_i - [T\beta \cdot ATP]_{i-1} \left( 1 - \frac{v}{V_0} \right) \right] \Delta H_{p1} \right. \\ &\quad + \left[ [T\beta \cdot Mg \cdot ATP]_i - [T\beta \cdot Mg \cdot ATP]_{i-1} \left( 1 - \frac{v}{V_0} \right) \right] (\Delta H_{p2} + \Delta H_{b1}) \\ &\quad + \left[ [Mg \cdot ATP]_i - [Mg \cdot ATP]_{i-1} \left( 1 - \frac{v}{V_0} \right) - F_{Mg \cdot ATP} [ATP]_0 \frac{v}{V_0} \right] \Delta H_{b1} \\ &\quad + \left[ [Mg_2 \cdot ATP]_i - [Mg_2 \cdot ATP]_{i-1} \left( 1 - \frac{v}{V_0} \right) \right. \\ &\quad \left. - F_{Mg_2 \cdot ATP} [ATP]_0 \frac{v}{V_0} \right] (\Delta H_{b1} + \Delta H_{b2}) \left. \right\} \end{aligned}$$

where  $\Delta H_{p1}$  and  $\Delta H_{p2}$  are the enthalpy changes associated with the binding of ATP and  $Mg \cdot ATP$  to  $T\beta$ , respectively, and  $\Delta H_{b1}$  and  $\Delta H_{b2}$  are the enthalpy changes associated with the binding of the first and second  $Mg(II)$  molecules to ATP, respectively. The correction terms including  $F_{Mg \cdot ATP}$  and  $F_{Mg_2 \cdot ATP}$ , the fractions of ATP in the syringe with one and two magnesium atoms bound,

Scheme 3



respectively, reflect the amount of  $Mg \cdot ATP$  and  $Mg_2 \cdot ATP$  complexes introduced into the cell just by injection and not due to equilibrium balance.

Finally, the heat effect is normalized considering the amount of ligand injected:

$$Q_i = \frac{q_i}{v[ATP]_0}$$

In the experiments,  $K_{b1}$ ,  $\Delta H_{b1}$ ,  $K_{b2}$ ,  $\Delta H_{b2}$ ,  $K_{P1}$ , and  $\Delta H_{P1}$  were determined directly from direct binary titrations.  $K_{P2}$  and  $\Delta H_{P2}$  were determined from the ternary experiments, once the other parameters had been previously determined.

The cooperativity in the binding of ATP and  $Mg(II)$  to  $T\beta$  is contained in the values of  $K_{P2}$  and  $\Delta H_{P2}$ . If  $K_{P1}$  and  $K_{P2}$  are equal and  $\Delta H_{P1}$  and  $\Delta H_{P2}$  are equal, the binding of  $Mg \cdot ATP$  to  $T\beta$  is the same as that of ATP, and magnesium does not have any effect on the ATP binding. If  $K_{P1}$  and  $K_{P2}$  are not equal and/or  $\Delta H_{P1}$  and  $\Delta H_{P2}$  are not equal, the binding of  $Mg \cdot ATP$  to  $T\beta$  is different from that of ATP, and magnesium has some effect on the ATP binding. In that case, the cooperative heterotropic association constant for ATP and magnesium binding to  $T\beta$  will be given by

$$\alpha = \frac{K_{P2}}{K_{P1}}$$

where an  $\alpha$  of  $> 1$  indicates positive cooperativity, an  $\alpha$  of  $< 1$  indicates negative cooperativity, and an  $\alpha$  of 1 indicates no cooperativity. Similarly, the cooperative enthalpy change for ATP and magnesium binding to  $T\beta$  will be given by

$$\Delta h = \Delta H_{P2} - \Delta H_{P1}$$

The cooperative entropy change can be calculated as

$$T\Delta s = \Delta h - \Delta g = \Delta h + RT \ln \alpha$$

Finally, we may conclude that the cooperative effect between  $Mg(II)$  and ATP is reciprocal. From energy conservation (Hess' law) applied to the formation of the  $T\beta \cdot Mg(II) \cdot ATP$  ternary complex, we obtain

$$K_{b1}K_{P2} = K_{P1}K_{b1}^*$$

$$\Delta H_{b1} + \Delta H_{P2} = \Delta H_{P1} + \Delta H_{b1}^*$$

then

$$\alpha = \frac{K_{P2}}{K_{P1}} = \frac{K_{b1}^*}{K_{b1}}$$

$$\Delta h = \Delta H_{P2} - \Delta H_{P1} = \Delta H_{b1}^* - \Delta H_{b1}$$

## REFERENCES

- Abrahams, J. P., Leslie, A. G. W., Lutter, R., and Walker, J. E. (1994) Structure at 2.8 Å resolution of F<sub>1</sub>-ATPase from bovine heart mitochondria. *Nature* 370, 621–628.
- Boyer, P. D. (1997) The ATP synthase: A splendid molecular machine. *Annu. Rev. Biochem.* 66, 717–749.
- Noji, H., and Yoshida, M. (2001) The rotary machine in the cell, ATP synthase. *J. Biol. Chem.* 276, 1665–1668.
- Adachi, K., Oiwa, K., Nishizaka, T., Furuie, S., Noji, H., Itoh, H., Yoshida, M., and Kinoshita, K., Jr. (2007) Coupling of rotation and catalysis in F<sub>1</sub>-ATPase revealed by single-molecule imaging and manipulation. *Cell* 130, 309–321.
- Miwa, K., and Yoshida, M. (1989) The  $\alpha_3\beta_3$  complex, the catalytic core of F<sub>1</sub>-ATPase. *Proc. Natl. Acad. Sci. U.S.A.* 86, 6484–6487.
- Dunn, S. (1980) ATP causes a large change in the conformation of the isolated  $\beta$  subunit of *Escherichia coli* F<sub>1</sub> ATPase. *J. Biol. Chem.* 255, 11857–11860.
- Hirano, M., Takeda, K., Kanazawa, H., and Futai, M. (1984) Detection of ATP-dependent conformational change in the F<sub>1</sub> portion and  $\beta$  subunit of *Escherichia coli* hydrogen-ATPase using 8-anilino-naphthalene-1-sulfonate. *Biochemistry* 23, 1652–1656.
- Odaka, M., Kaibara, C., Amano, T., Matsui, T., Muneyuki, E., Ogasahara, K., Yutani, K., and Yoshida, M. (1994) Tyr-341 of the  $\alpha$  subunit is a major Km-determining residue of TF<sub>1</sub>-ATPase: Parallel effect of its mutations on Kd(ATP) of the  $\alpha$  subunit and on Km(ATP) of the  $\alpha_3\beta_3\gamma$  complex. *J. Biochem.* 115, 789–796.
- Jault, J., Kaibara, C., Yoshida, M., Garrod, S., and Allison, W. S. (1994) Probing the specificity of nucleotide-binding to the F<sub>1</sub>-ATPase from thermophilic *Bacillus PS3* and its isolated  $\alpha$  and  $\beta$  subunits with 2-N<sub>3</sub>-( $\beta$ , $\gamma$ -<sup>32</sup>P)-ATP. *Arch. Biochem. Biophys.* 310, 282–288.
- Yagi, H., Tozawa, K., Sekino, N., Iwabuchi, T., Yoshida, M., and Akutsu, H. (1999) Functional conformation changes in the TF<sub>1</sub>-ATPase subunit probed by 12 tyrosine residues. *Biophys. J.* 77, 2175–2183.
- Yagi, H., Tsujimoto, T., Yamazaki, T., Yoshida, M., and Akutsu, H. (2004) Conformational change of H<sup>+</sup>-ATPase  $\beta$  monomer revealed on segmental isotope labeling NMR spectroscopy. *J. Am. Chem. Soc.* 126, 16632–16638.
- Yagi, H., Kajirawa, N., Iwabuchi, T., Izumi, K., Yoshida, M., and Akutsu, H. (2009) Stepwise propagation of the ATP-induced conformational change of the F<sub>1</sub>-ATPase  $\beta$  subunit revealed by NMR. *J. Biol. Chem.* 284, 2374–2382.
- Kayalar, C., Rosing, J., and Boyer, P. D. (1977) An alternating site sequence for oxidative phosphorylation suggested by measurement of substrate binding patterns and exchange reaction inhibitions. *J. Biol. Chem.* 252, 2486–2491.
- Bianchet, M. A., Hüllihen, J., Pedersen, P. L., and Amzel, L. M. (1998) The 2.8-Å structure of rat liver F<sub>1</sub>-ATPase: Configuration of a critical intermediate in ATP synthesis/hydrolysis. *Proc. Natl. Acad. Sci. U.S.A.* 95, 11065–11070.
- Gibbons, C., Montgomery, M. G., Leslie, A. G. W., and Walker, J. E. (2000) The structure of the central stalk in bovine F<sub>1</sub>-ATPase at 2.4 Å resolution. *Nat. Struct. Biol.* 7, 1055–1061.
- Rodgers, A. J. W., and Wilce, M. C. J. (2000) Structure of the  $\gamma$ - $\epsilon$  complex of ATP synthase. *Nat. Struct. Biol.* 7, 1051–1054.
- Braig, K., Menz, R. I., Montgomery, M. G., Leslie, A. G. W., and Walker, J. E. (2000) Structure of bovine mitochondrial F<sub>1</sub>-ATPase inhibited by Mg<sup>2+</sup>ADP and aluminium fluoride. *Structure* 8, 567–573.
- Menz, R. I., Walker, J. E., and Leslie, A. G. W. (2001) Structure of bovine mitochondrial F<sub>1</sub>-ATPase. *Cell* 106, 331–341.
- Chen, C., Saxena, A. K., Simcoke, W. N., Garboczi, D. N., Pedersen, P. L., and Ko, Y. H. (2006) Mitochondrial ATP synthase. Crystal structure of the catalytic F<sub>1</sub> unit in a vanadate-induced transition-like state and implications for mechanism. *J. Biol. Chem.* 281, 13777–13783.
- Kabaleeswaran, V., Puri, N., Walker, J. E., Leslie, A. G. W., and Mueller, D. M. (2006) Novel features of the rotary catalytic mechanism revealed in the structure of yeast F<sub>1</sub> ATPase. *EMBO J.* 25, 5433–5442.
- Bowler, M. W., Montgomery, M. G., Leslie, A. G. W., and Walker, J. E. (2007) Ground state structure of F<sub>1</sub>-ATPase from bovine heart mitochondria at 1.9 Å resolution. *J. Biol. Chem.* 282, 14238–14242.
- Kabaleeswaran, V., Shen, H., Symersky, J., Walker, J. E., Leslie, A. G. W., and Mueller, D. M. (2009) Asymmetric structure of the yeast F<sub>1</sub> ATPase in the absence of bound nucleotides. *J. Biol. Chem.* 284, 10546–10551.
- Ko, Y. H., Hong, S., and Pedersen, P. L. (1999) Chemical mechanism of ATP synthase. *J. Biol. Chem.* 274, 28853–28856.
- Weber, J., Hammond, S. T., Wilke-Mounts, S., and Senior, A. E. (1998) Mg<sup>2+</sup> coordination in catalytic sites of F<sub>1</sub>-ATPase. *Biochemistry* 37, 608–614.
- Nadanaciva, S., Weber, J., and Senior, A. E. (1999) Binding of the transition state analog MgADP-fluoroaluminate. *J. Biol. Chem.* 274, 7052–7058.
- Milgrom, Y. M., and Cross, R. L. (2005) Nucleotide binding sites on beef heart mitochondrial F<sub>1</sub>-ATPase. *Proc. Natl. Acad. Sci. U.S.A.* 102, 13831–13836.
- Bulygin, V. V., and Milgrom, Y. M. (2007) Studies of nucleotide binding to the catalytic sites of *Escherichia coli*  $\beta$ Y331W-F<sub>1</sub>-ATPase using fluorescence quenching. *Proc. Natl. Acad. Sci. U.S.A.* 104, 4327–4331.
- García, J. J. (2000) The F<sub>0</sub>F<sub>1</sub>-ATP synthase: Binding energy, coupling and rotational catalysis. *Recent Res. Dev. Bioenerg.* 1, 41–62.

29. Böckmann, R. A., and Grubmüller, H. (2002) Nanoseconds molecular dynamics simulation of primary mechanical energy transfer steps in F<sub>1</sub>-ATP synthase. *Nat. Struct. Mol. Biol.* 9, 198–202.
30. Pérez-Hernández, G., García-Hernández, E., Zubillaga, R. A., and Tuena de Gómez-Puyou, M. (2002) Structural energetics of MgADP binding to the isolated  $\beta$  subunit of F<sub>1</sub>-ATPase from thermophilic *Bacillus PS3*. *Arch. Biochem. Biophys.* 408, 177–183.
31. Wiseman, T., Williston, S., Brandts, J. F., and Lin, L. N. (1989) Rapid measurement of binding constants and heats of binding using a new titration calorimeter. *Anal. Biochem.* 179, 131–137.
32. Hammann, C., Cooper, A., and Lilley, D. M. J. (2001) Thermodynamics of ion-induced RNA folding in the hammerhead ribozyme: An isothermal titration calorimetric study. *Biochemistry* 40, 1423–1429.
33. Luque, I., and Freire, E. (1998) Structure-based prediction of binding affinities and molecular design of peptide ligands. *Methods Enzymol.* 295, 100–135.
34. Chavelas, E. A., and García-Hernández, E. (2009) Heat capacity changes in carbohydrates and protein-carbohydrate complexes. *Biochem. J.* 420, 239–247.
35. Marcus, Y. (1994) A simple empirical model describing the thermodynamics of hydration of ions of widely varying charges, sizes, and shapes. *Biophys. Chem.* 51, 111–127.
36. Makhatadze, G. I., and Privalov, P. L. (1992) Contribution of hydration and non-covalent interactions to the heat capacity effect on protein unfolding. *J. Mol. Biol.* 224, 715–723.
37. Smith, R. M., Martell, A. E., and Chen, Y. (1991) Critical evaluation of stability constants for nucleotide complexes with protons and metal ions and the accompanying enthalpy changes. *Pure Appl. Chem.* 63, 1015–1080.
38. Wilson, J. E., and Chin, A. (1991) Chelation of divalent cations by ATP, studied by titration calorimetry. *Anal. Biochem.* 193, 16–19.
39. Alberty, R. A. (1969) Maxwell relations for thermodynamics quantities of biochemical reactions. *J. Am. Chem. Soc.* 91, 3899–3903.
40. Wang, P., Oscarson, J. L., Izatt, R. M., Watt, G. D., and Larsen, C. D. (1995) Thermodynamic parameters for the interaction of adenosine 5'-diphosphate, and adenosine 5'-triphosphate with Mg<sup>2+</sup> from 323.15 to 398.15 K. *J. Solution Chem.* 24, 989–1012.
41. Dou, C., Fortes, G., and Allison, W. S. (1998) The  $\alpha_3(\beta\gamma 341W)_3\gamma$  subcomplex of the F<sub>1</sub>-ATPase from the thermophilic *Bacillus PS3* fails to dissociate ADP when MgATP is hydrolyzed at a single catalytic site and attains maximal velocity when three catalytic sites are saturated with MgATP. *Biochemistry* 37, 16757–16764.
42. Weber, J., and Senior, A. E. (2000) ATP synthase: What we know about ATP hydrolysis and what we do not know about ATP synthesis. *Biochim. Biophys. Acta* 1458, 300–309.
43. Prabhu, N. V., and Sharp, K. A. (2005) Heat capacity in proteins. *Annu. Rev. Phys. Chem.* 56, 521–548.
44. Ladbury, J. E., and Williams, M. A. (2004) The extended interface: Measuring non-local effects in biomolecular interactions. *Curr. Opin. Struct. Biol.* 14, 562–569.
45. Bello, M., Pérez-Hernández, G., Fernández-Velasco, D. A., Arreguín-Espinosa, R., and García-Hernández, E. (2008) Energetics of protein homodimerization: Effects of water sequestering on the formation of  $\beta$ -lactoglobulin dimer. *Proteins: Struct., Funct., Bioinf.* 70, 1475–1487.
46. Wilcox, D. (2008) Isothermal titration calorimetry of metal ions binding to proteins: An overview of recent studies. *Inorg. Chim. Acta* 361, 857–867.
47. Velazquez-Campoy, A., Goñi, G., Peregrina, J. R., and Medina, M. (2006) Exact analysis of heterotropic interactions in proteins: Characterization of cooperative ligand binding by isothermal titration calorimetry. *Biophys. J.* 91, 1887–1904.
48. Martínez-Julvez, M., Medina, M., and Velazquez-Campoy, A. (2009) Binding thermodynamics of ferredoxin:NADP<sup>+</sup> reductase: Two different protein substrates and one energetics. *Biophys. J.* 96, 4966–4975.
49. Amzel, L. M. (1997) Loss of translational entropy in binding, folding, and catalysis. *Proteins: Struct., Funct., Genet.* 28, 144–149.
50. Dong, K., Ren, H., and Allison, W. S. (2002) The fluorescence spectrum of the introduced tryptophans in the  $\alpha_3(\beta F155W)_3\gamma$  subcomplex of the F<sub>1</sub>-ATPase from the thermophilic *Bacillus PS3* cannot be used to distinguish between the number of nucleoside di- and triphosphates bound to catalytic sites. *J. Biol. Chem.* 277, 9540–9547.
51. Weber, J., and Senior, A. E. (2001) Bi-site catalysis in F<sub>1</sub>-ATPase: Does it exist? *J. Biol. Chem.* 276, 35422–35428.
52. Yasuda, R., Masaike, T., Adachi, K., Noji, H., Itoh, H., and Kinoshita, K., Jr. (2003) The ATP-waiting conformation of rotating F<sub>1</sub>-ATPase revealed by single-pair fluorescence resonance energy transfer. *Proc. Natl. Acad. Sci. U.S.A.* 100, 9314–9318.
53. Zheng, W. (2009) Normal-mode-based modeling of allosteric couplings that underlie cyclic conformational transition in F<sub>1</sub> ATPase. *Proteins: Struct., Funct., Bioinf.* 76, 747–762.
54. Weber, J., and Senior, A. E. (2004) Fluorescent probes applied to catalytic cooperativity in ATP synthase. *Methods Enzymol.* 380, 132–152.
55. Bandyopadhyay, S., Valder, C. R., Huynh, H. G., Ren, H., and Allison, W. S. (2002) The  $\beta G156C$  substitution in the F<sub>1</sub>-ATPase from the thermophilic *Bacillus PS3* affects catalytic site cooperativity by destabilizing the closed conformation of the catalytic site. *Biochemistry* 41, 14421–14429.